Speculation of Sn-Zn Alloy and Borosilicate-Bismuth glass on IR inhibition and Thermal performance of Polysiloxane Coatings

Junhong Hu

Hong Kong Metropolitan University, HongKong,999077, China

Abstract. The low infrared emissivity coating was formulated based on the use of the Sn-Zn (70:30) low melting alloy powder as the infrared functional filler, polysiloxane powder as organic binder, and the B_2O_3-SiO_2-Bi_2O_3 poly component Glass coating powder, which served as the inorganic binder, respectively. The compositional and structural change of the coating to high temperature treatment was determined using thermogravimetric, Fourier transform infrared spectroscopy, thermo-mechanical analyzer, and field emission scanning electron microscope. In addition, the process of the influence of high temperature-induced composition change on the mechanical behavior of the coating was extensively analyzed, and the parameters in the wind erosion resistance temperature field were tested by using a homemade apparatus. According to the findings, the infrared emissivity of the coating reached a minimum of 0.26 (in 8-14 microns), as determined at 580° C, and this was attributable to decomposition of polysiloxane, rearrangement of the surface of Sn-Zn alloys particles, and pore closure that resulted from the influence on glass softening. Further, thermal pretreatment was specifically favorable to remove shrinkage stresses caused by polymer decomposition, as well as promoting enhanced melting diffusion of Bi_2O_3-rich glass in the range between 400 °C and 520 °C. The resistance to wind erosion became significantly more resistant even when subjected to a pretreatment of 500-600° C as well. The coating can also be used as an energy-efficient surface, and because of its highest infrared radiation blocking property, very high thermo-protective capability, and high mechanical strength due to high temperature erosion-resistant quality.

Keywords: Sn-Zn Alloy; Borosilicate-Bismuth glass; low infrared emissivity coating.

1. Introduction

Low infrared-emissive (low-E) organic-inorganic glassy hybrid coatings have witnessed wide interest in thermal insulation, fire-protective, and infrared camouflage applications because they are inexpensive, easily manufactured, and highly maintainable.[1] These are also the coatings that are widely applicable in fire-resistance use, whereby they help to protect other structures behind them in the face of external heating radiation. [2]

Thermal stability of organic/inorganic coatings is also a broad area of investigation in order to achieve the best performance of coatings at high temperatures in terms of protection.[3] Low infrared-emitting coating with good flame resistance has been demonstrated to minimize radiative heat transfer, thus offering better protection of the substrates under thermal pressure. Multi-layered thin coating structures that integrate sub-micrometer in-reflective IR layers with low surface absorption were found to be effective in both preventing the oxidative processes and mitigating, by reducing, the flammability spread.[5] In addition, proper real-time temperature measurements are central to knowing the pyrolysis characteristics of polymers and the processes that lead to their flame retardancy. The impact of displayed radiation upon the coating surface is one of the major factors that contribute to the effectiveness of the coating to block thermal energy. Thus, when placed under high-speed and high-temperature conditions of the heat flow, it is imperative to determine the infrared suppressing and thermal protection behavior of the low-E organic/inorganic coatings applied at an actual operating temperature.[7]

Organic/inorganic composite coatings emerge as an exciting area of study because they ought to be thermally stable, in addition to having low infrared emissive properties.[8] Xu et al. reviewed the studies on polysiloxane elastomer-based polyurethanes and identified that the aliphatic and aromatic diisocyanate chemistries affect the thermal degradation and surface thermal stability based on the thermo-gravity (TG) and spectroscopic investigation; however, they did not discuss the aluminum and glass-powder-thin-films-coated papers in real high-temperature oxidizing conditions.[9] They are very desirable due to their optical properties, but are very easily degraded when exposed to temperatures above 500 ° C, and do not exhibit good thermal shock properties. Reportedly, the primary cause of such performance is associated with both the thermal breakdown of the polysiloxane-based matrix and the oxidation of aluminum particles that collectively undermine the design of the interfaces and increase the infrared reflectivity. [10] The works of Fang et al. studied infrared-stealth nanofibrous composites based on a combination of polymer and inorganic fillers, with improved thermal stability and low emissivity being shown during tests on mechanical flexibility and thermal cycling, but their system is not an aluminum/polysiloxane/glass hybrid with continuous exposure to high temperatures.[11] Upon exposure to thermal treatment, an increase in bond strength and mechanical response has been noted, but most of those tests were done with the post-cooling treatment and, therefore, with insufficient coverage of the dynamic behavior of the material under the actual operation at high temperatures. In fact, in the real world, during the deposition process of thermal-oxidative breakdown of polysiloxane, oxidation of metallic fillers and stepwise softening or fusing of glass powders are superposed processes that have the possibility of modifying the composition, microstructure, and spectral emission properties of the coating in real time. The prospects of all these transmutations are essential to the fashioning of an envelope, which will be able to maintain low reflectivity and mechanical balance against certain permanent thermal stress.

In an attempt to enhance the comprehensive behavior of coatings in response to exposure to high temperatures, various experimental methods have been established that involve real-time thermal monitoring using in-situ temperature-tracking methods.[12] The approaches are good in giving guidance on the quick screening and design of high-performance, heat-resistant materials. It has also been noted that the fire-retardant and thermal-protecting capacity of composite constituents can be greatly derailed by the thermal decomposition manner and rheology of those constituents. In the case of polysiloxane coating, the IR emissivity and the constancy of the mechanics are devastatingly susceptible to dynamic thermal conditions. In high-temperature heat flow or high-speed flights, when the rates of different components of the thermal decomposition of the polysiloxane matrix vary in different ranges, when metallic fillers are completely oxidized or glass components are melting, it is possible to observe significant changes in the surface structure, emissivity, and mechanical strength. Specifically, the degradation of the polymer binder and the thermophysical process of metal and glass phases are most critical in regulating the capacity of the coating to retain thermal protection and integrity. Khurana et al. confirmed that EPDM is the most suitable polymeric binder to develop coating formulations for radioactive waste storage containers when compared with PU, HDPE, and epoxy.[13] Although earlier works have been carried out on low-emissivity coating systems, there is hardly any research done to study the infrared and mechanical properties in real time during prolonged exposure to high temperatures and vibrations.[14] The interaction between the degradation of the polymers, the oxidation or rearrangement of alloy particles, and the softening or bonding of the glass powder is not well known. Thus, the study of the co-evolution of these processes and how they govern the performance of coatings at high temperatures is necessary to develop infrared-stealth and thermal-protection coatings of the next generation.

The major aim of the research problem here is to determine the effect of the high-temperature infrared suppression, fire protection, and wind erosion resistance (WER) of polysiloxane-based coating reinforced with Sn-Zn alloy and multicomponent glass powder of B_2O_3-SiO_2-Bi_2O_3. To understand the mechanism of the effect of compositional evolution on the infrared performance of the coating during heating and subsequent cooling, a set of thermal analysis experiments was conducted to measure the in-situ changes of a) the matrix that constitutes the polysiloxane, b) the Sn-Zn alloy particles, and c) the glass fillers at high temperatures. There was special focus on the internalization of how the softening and bonding nature of the glass powder impacts the structural rearrangement of the metallic alloy at high temperatures, and consequently, what is going to influence the surface morphology and the infrared reflectivity. Theoretical and experimental analyses of changes in the structure of the coating (surface roughness and gloss) were made to establish their influence on the reflection and scattering of the incident infrared radiation. In addition, the overall thermal dimensional stability of the coating in relation to the substrate under actual high-temperature regimes was examined in detail to evaluate the effect of possible stress build-up and interface bias. High fidelity, designed in the form of a naturally varied experiment, was utilised to systematically assess the WER behaviour of the low-emissivity coatings developed, and this was vital in the design of IR stealth systems and thermo-protection surfaces of high-speed aerospace vehicles.

2. Experimental procedures

2.1 Experimental materials

The methyl-phenyl polysiloxane was given by Hubei Longsheng Sihai New Material Co., Ltd. (China), and it was used as an organic binder due to its high thermal stability and good film-forming property. B2O3-SiO2-Bi2O3 inorganic powder was B2O3-SiO2-Bi2O3 glass powder, inorganic binder manufactured by Hunan Nuoli New Material Co., Ltd. (China), its softening temperature was around 390 ° C. Being the low-emissivity functional filler, the alloy was bound to an inexpensive spherical Sn-Zn alloy of medium particle sizes (~20 μm) and a balance of visibility (70:30 (Sn: Zn)), supplied by the Shanghai Epiom Materials Technology Co., Ltd. (China). Modification of coating viscosity and obtaining a homogenous dispersion of the coating were carried out in the organic solvent, which is a mixture of butyl acetate and xylene, both acquired at Chengdu Kelong Chemical Co., Ltd. (China).

2.2 Preparation of Coatings

To begin with, 13.2 g of B_2O_3-SiO_2-Bi_2O_3 glass powder and 30 g of methyl-phenyl polysiloxane were added to a mixture of butyl acetate and xylene and stirred statistically with the aid of a magnet in order to come up with uniform mixing during a period of 360 minutes at the rate of approximately 1000 rpm. After that, 45 grams of Sn-Zn alloy powder (Sn: Zn = 70:30, mass ratio) were added to the suspension slowly, and the suspension was further stirred at 500 rpm for another 10 minutes till a homogeneous distribution of the metallic filler was accomplished. The slurry so formed was laid in turn on the surfaces of treated stainless steel (dimension: 60 mm x 50 mm x 0.3 mm) utilizing an air spray method. Flows of water curtain and gas filtration circulation were used in the process of spraying to provide a clean operating environment. Upon application, the samples with coating were placed in an oven and dried under the conditions of 60 ° C, 6 h to remove the remaining solvent, and then cured at 200 ° C for 2 h to induce the crosslinking of the polysiloxane network and incomplete fusion of the glass phase. The last layer was formed of Sn-Zn alloy, polysiloxane, and glass powder (the mass ratio of metal to polymer was 1.5:1, and the content of glass was ~15% wt.% %) and marked as SZG coating to be characterized and tested later.

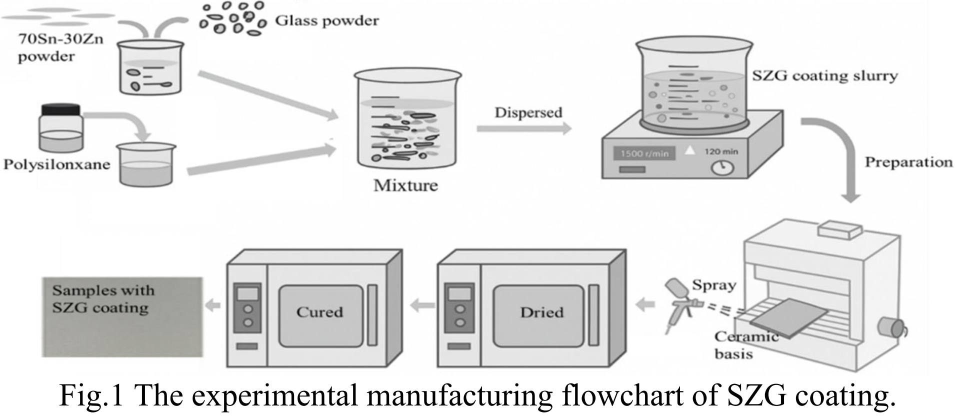

Fig.1 The experimental manufacturing flowchart of SZG coating.

2.3 Wind Erosion Resistance Testing

In order to test the mechanical evolution temperature effect on the wind erosion resistance (WER) of the coating, samples were put into the muffle furnace and pretreated following three steps: Step 1: preheated to the temperatures between 200 and 600° C (tested at 250, 300, 350, and 400° C and 500 and 600° C) in the muffle furnace with a time of 20 min; Step 2: cooled naturally to room temperature. The rate of motion of the nozzle in the lateral direction was to be 5 cm/s to have the same proportionality of exposure. The pressure of shock was maintained at the range of 10-11 kPa. Mixing of gas was done within the temperature range of 650-700 ° C; in this way, the gradual temperature rise of the surface was measured because of the overall cyclic thermal-mechanical loading requirement of the gaseous materials in the surface of the coating. Erosion temperature was checked by a temperature detector in real time at the surface where it was measured. Optical microscopy was also used to ascertain whether there were any morphological changes and the development of damage after every exposure period. The WER threshold temperature of the coating was selected as the critical temperature when the damage of the surface started to develop.

2.4 Characterization

Field emission scanning electron microscopy (FE-SEM, FEI Inspect F50) and optical microscopy (KL-1000, 20X and 100X magnifications) were used to analyze the surfaces of coatings in terms of particle dispersion, the compactness of the surfaces, and any evidence of damage. Thermal and chemical transformations in coatings were evaluated using one thermogravimetric analysis and differential scanning calorimetry analysis (TG/DSC) performed with Netzsch STA 449F3 equipment in the atmosphere of ambient air at a heating rate of 10 ° C per minute. In order to check the optical qualities and surface texture, the roughness meter and the gloss meter (BYKR 4561 micro-TRI-gloss) were used to measure the roughness and surface glossiness. The infrared optical properties were measured by Fourier transform infrared (FTIR, Bruker Tensor 27) to measure the reflectance and the transmittance of the spectra of FTIR. The temperature on the surface could be measured in real time by placing temperature detectors (TRSI TA612C) on the surface during testing on gas erosion or heating, or by measuring the temperature of the radiation of infrared radiation (FLIR T1050).

3. Results and Discussion

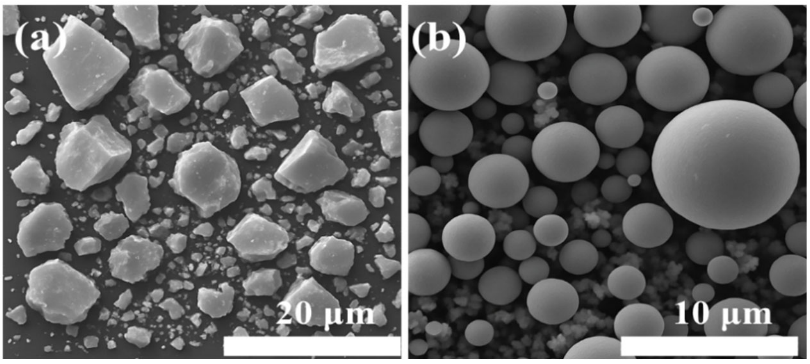

Fig.2 SEM morphologies of (a) BSB glass powders;(b) Sn-Zn alloy powder.

The two key solid fillers applied to the SZG coating have morphologies that can be seen in Figure 2. In Figure 2(a), the B2O3-SiO2-Bi2O3 (BSB) multicomponent glass powders are uneven and sharp in the geometrical aspect, having a broad particle size range containing sub-micrometer pieces up to around 20 μm agglomeration. The resultant morphological diversity promotes effective interparticle sintering and flows during thermal treatment and thereby facilitates structural densification of the coating and the potential to partially fill in the pores within a coating matrix at high temperatures. On the contrary, Figure 2(b) will show Sn-Zn (70:30) alloy powders where the particles are very spherical and smooth in their surface and with a particle size of 15-20 μm. Because of its spherical shape, which is characteristic of the gas-atomized production process, the material disperses evenly in the polymer, and the stress concentrations are low. In addition, the low melting temperature of SnZn alloy (ca. 198 ° C) and its concave shape facilitate rearrangement and sintering effects under average heating conditions that result in reflectivity adjustment and lowering of emissivity during high temperature test exposure.

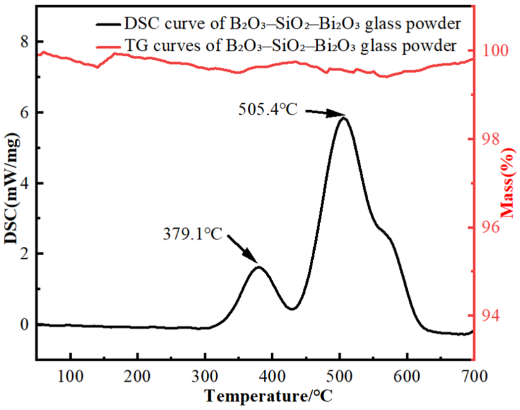

Fig.3 DSC-TG curves of B2O3-SiO2-Bi2O3 powders.

Figure 3 shows the thermogravimetric (TG) and the evaluation of the B_2O_3-SiO_2-Bi_2O_3 multicomponent glass powders using the differential scanning calorimetry (DSC). As shown in the TG curve (red), the loss in mass is minimal, and no more than 6 percent is lost as the temperature range (25-700 ° C) increases. The respective DSC graph (black) reveals that there are two endothermic peaks, which are observed at 379.1 and 505.4°C, respectively. The component with the low melting point of B_2O_3 has a direct effect on the area close to the major peak detected at approximately 379°C of the end product, which is a glass transition or softening point of that multicomponent mixture. The in-situ development of the coating microstructure can be significantly comprehended as a matter of these thermal events. In particular, the temperature range of softening (380-520 ° C) is found on the decomposition phase of the polysiloxane binder at the rearrangement phase of the Sn-Zn alloy particles. This synchronized time will lead the softened glass to invade the pores and bond to the metallic filler plates to provide a densification to the structural material and a bond across the interface in the SZG layer coating. Also, the lack of exothermic crystallization peaks justifies using this type of glass as a stable amorphous additive to high-temperature morphology control without inducing phase instability. Generally, the thermal property of the BSB glass powder is essential, and this has led to improved infrared reflectivity and wind erosion capabilities since they undergo a microstructural reconfiguration, as a result of heat treatment.

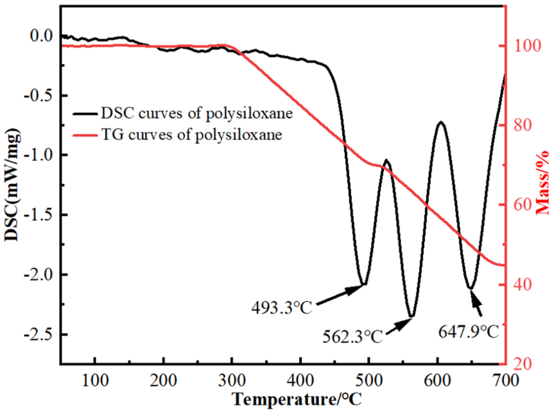

Fig.4 DSC-TG curves of polysiloxane.

In Figure 4, thermo-gravimetric (TG) and differential scanning calorimetric (DSC) thermograms of the methyl-phenyl polysiloxane in an oxidative atmosphere were presented, showing a complicated multiple-stage process of decomposition. The TG curve (red) shows that, first of all, it starts to lose its mass around 300° C and then undergoes a gradual, more significant stage of decomposition (400°

C to 650° C) where the remaining mass of the material reduces to around 40 percent. The latter was supposed to be most frequently accounted for by successive oxidative cleavage of terminal hydroxyl groups, methyl/ phenyl side chains, and further purification of the siloxane and backbone. At the same time, the DSC curve (black) demonstrates three unique exothermal peaks of 493.3° C, 562.3° C, and 647.9° C with the processes of step-by-step degradation of the polymer. These are side group oxidation, chain scission, and lastly the rearrangement and oxidation of the siloxane network into stable, thermally silica-like residues. The range of softening temperature of glass (B_2O_3-SiO_2-Bi_2O_3) overlaps with the point of thermal degradation to a significant extent, which means that due to polysiloxane degradation, one can fill the pores with softened glass (Figure 3). This increases densification and building up of the structure in the composite coating. The multi-peak exothermic profile suggests that the amount of local heat release and shrinkage is high, and the intensity of these peaks has to be controlled with thermal pre-treatment so that the mechanical stability and crack resistance can be maintained at elevated temperatures.

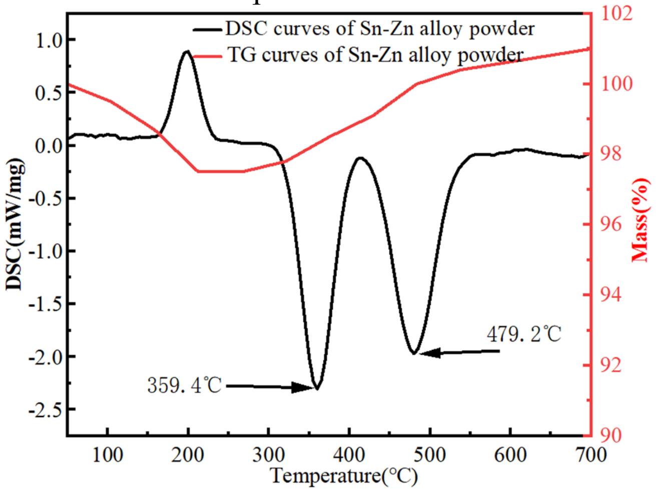

Fig.5 DSC-TG curves of Sn-Zn alloy powders.

The DSC-TG curves of Sn-Zn (70:30) alloy powder are shown in Figure 5, which depicts the various thermal events that happen to this material in the presence of an oxidative environment. According to the corresponding differential scanning calorimetry (DSC) curve (black), there are two significant thermal processes: endothermic valley at 359.4 ℃, which can be related to eutectic melting of the Sn-Zn alloy system and a broader one endothermic peak at 479.2 °C, which can be attributed to phase separation and internal rearrangement of alloy constituents in molten alloy under partial oxidation process. This characteristic of low-temperature eutectic melting (~359°C) is one of the major differences between Sn-Zn and the traditional Al fillers, and also the ability to experience early-stage softening and flow on the surface upon exposure to elevated temperatures. In the meantime, the fact that only a small mass accumulation is seen in the TG curve indicates that there was not a great deal of oxidation of Sn and Zn, and an oxide coating (thin oxide shell) may be formed, which simultaneously preserves the morphology of particles without severely affecting the reflectivity. The Sn-Zn alloy under review can be compared to the Al powder in the reference system in terms of lower melting temperature, less aggressive oxidation chemistry, and the ability to blend well into low-viscosity glass, which results in the advantageous ease of microstructural evolution and emissivity management in the 350-500 °C range.

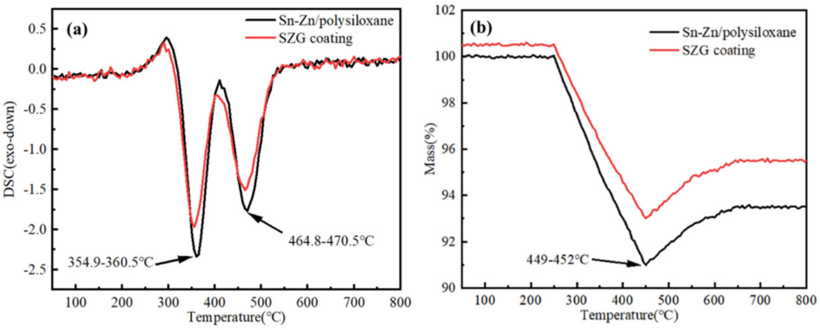

Fig.6 DSC-TG curves of Sn-Zn/polysiloxane and SZG coating.

The difference between the properties of the Sn-Zn/polysiloxane binary system and that of the entire SZG composite coating with regard to the differential scanning calorimetry (DSC) and thermogravimetric (TG) response is made as a comparison of the thermal properties (Figure 6). As Figure 6 (a) indicates, in the two systems, respectively, 2 different peaks are discerned by the DSC. The two peaks that come out at 354.9-360.5℃ and 464.8-470.5℃ can be attributed to eutectic melting of Sn-Zn alloy and thermic decomposition of polysiloxane and subsequent reorganization of structure, respectively. Nevertheless, the SZG coating (red curve) had a smaller magnitude loss of mass and more remaining mass with respect to deposit temperature, implying a greater level of thermal stability. This can likely be attributed to the incorporation of B2O3 -SiO2 -Bi2O3 glass powder, which is softened and melted at relatively similar temperatures in order to occupy the pores, and it lends some strength to the structure against any wear and tear that may take place due to refrigeration. The synergy of the SZG system concentrates on the effective interaction among metallic softening, the breaking down of polymers, and the softening of glass. Such a well-stacked order may be rearranged in the dynamical process of heating, and that will cause densification and stability of the coating. Such changes are crucial to ensure low infrared emissivity and/or mechanical integrity of high-temperature operation, especially in the aerospace environment or the thermal stealth environment.

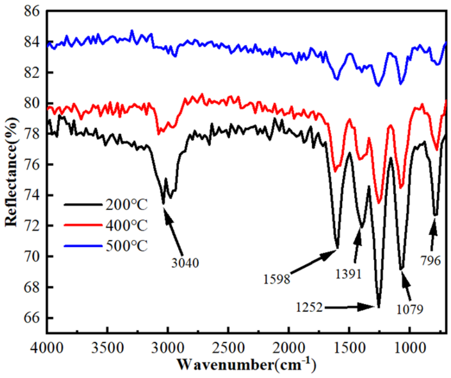

Fig. 7 FTIR reflectance spectrum of the SZG coating at different temperatures.

Figure 7 shows the Fourier-transform infrared (FTIR) reflectance spectra of SZG composite coating as measured at 200 °C, 400 °C, and 500 °C of the mid-infrared limiting range (4000-400 cm-1). At each temperature, differences are observed in the spectra that indicate specific absorption bands, which are characteristic of the various functional groups within the polysiloxane binder material and also of species present on the surfaces. It is observed that on increasing the temperature, an apparent tendency of increasing upward trend in the overall reflectance is evident, and in particular after a temperature of 400 ° C. Such behaviour is strongly related to the thermally induced decomposition of organic parts and surface remodelling of the coating. Decreasing absorption peaks around 3040 cm^{-1} and 1391 cm^{-1} at 500°C show that methyl and phenyl groups of the polysiloxane matrix are becoming degraded. At the same time, the increase in the baseline reflectance in the atmospheric window of 8 14 14 (1250 714 19 cm -1) can be seen as evidence of the less disturbed surface topography and higher infrared reflectivity. The spectral evolution affirms that chemical and structural changes, i.e., polymer decomposition process, glass flow, and alloy rearrangement, are incorporated in high-temperature treatment, which together result in low infrared absorption and stealth. SZG coating (treated at 500 °C) has the best spectral reflectance characteristics and hence may be performed when a coat is desired to control the thermal-related concealment or emissivity at elevated conditions.

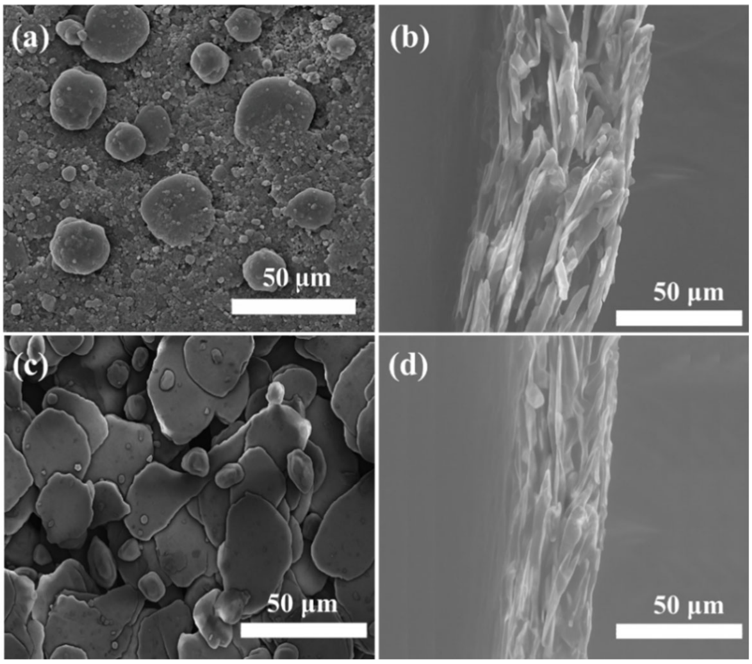

Fig. 8 SEM images of the SZG coating. (a) 200 °C and (c) 500 °C corresponding to the top view of the surface, (b) 200 °C and (d) 500 °C corresponding to the cross-sectional view.

Figure 8 indicates SEM micrographs of a cross-section and also on the surface of the SZG composite coating before and after the thermal treatment, and it presents the morphological change of both surface structures and the cross-section. With that low temperature, the surface is made up of loose packed, rounded Sn-Zn alloy particles with definite interparticle space. In the cross-section (b), its architecture is porous and packed, and the flow of the binder and poor interfacial adhesion between fillers are not good. The surface (c) is significantly denser, and the particles are incorporated and flattened, which perhaps conveys the idea that the surface of the Sn-Zn alloy has rearranged, and there is some glass flow, as well. At the same time, the cross-sectional picture (d) shows the densification of the stratification and the reduced interstitial flaws, which implies the intensification of the interphase bonding and the consolidation of the structure because of the softening and wetting nature of the B_2O_3-SiO_2-Bi_2O_3glass. Such thermal-based densification process not only enhances the cohesion and mechanical strength of the coating but also leads to smoothing of the surface and reduction of infrared emissivity. The morphological change supports FTIR and DSC-TG data, indicating that the 500°C treatment is the best option for attaining the integration of the thermal protection and infrared stealth capability. These findings confirm the synergetic effect of decomposition of the polymers, remodeling of the alloys, and liquidation of the glass in the production of a dense and strong coating at high temperatures.

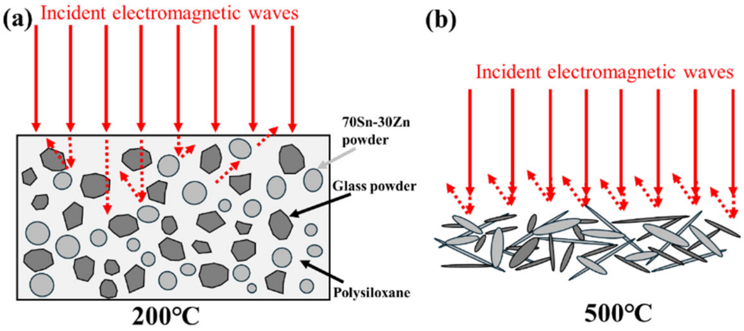

Fig. 9 Diagram of the model of the coating structure.

Figure 9 is a conceptual map of the development process of microstructure and electromagnetic interaction of SZG composite coating at a temperature of 200°C and 500°C. A loose filled SnZn alloy powder (particles), angular broken pieces of glass destiny and unreacted polysiloxane can be taken to get the glass at low temperatures (200 o C) and the coating in panel (a). The random shape and the scattered spatial pattern atypicality reinvent increased surface roughness and poor reflection rate, thus lowering the infrared suppression potential in the coating. On a comparative level, panel (b) qualifies the rearranged morphology at 500°C after the thermal degradation of polysiloxane upon the melting of the $(B_2O_3)SiO_2$-Bi_2O_3-glass. The schematic is quite representative of the functional transformation of a disordered, highly absorptive microstructure to ordered, reflective architecture as in the case of SEM (Fig. 8) and FTIR (Fig. 7). Transformation verifies that synergistic effect of alloy rearrangement and flow of glass at 500°C is needed to ensure minimum infrared emissivity and perfect stealth performance of the coating. The given model emphasises the significance of temperature-conditioned structural modulation towards the realisation of tuneable infrared suppressions within the context of multifunctional thermal protective coatings.

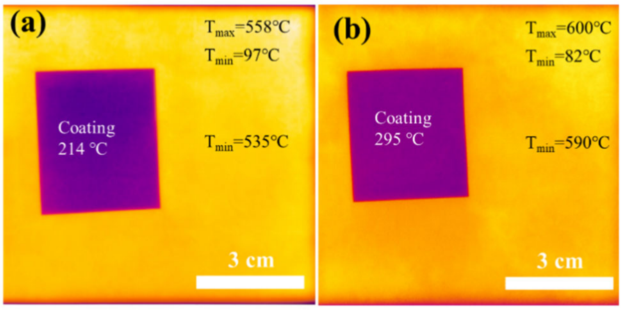

Fig. 10 Temperature of the ceramic plate and the SZ G coating infrared radiation (a) 570°C. and (b) 620 °C.

Infrared thermal images of the radiation behavior of the SZG coating at high temperature and that of a bare ceramic substrate at high temperature, the comparator is provided in figures 10 (a) and 10 (b) at 570 and 620 degrees centigrade, respectively. The surface radiation temperature of the ceramic plate is also found to be much higher in both incidences, with readings of 535-558 ℃ and 590-600℃, respectively. The middle-zone, however, coincides with that of the SZG coating and is considerably cooler, with surface temperature being recorded to be 214° C and 295° C. The comparatively low apparent temperature of the SZG coating, under the same heating conditions, is attributed to its designed microstructure with low-emitting particles of Sn-Zn alloys and a densified surface topography after being thermally processed. In addition to the advantage associated with this thermal effect, the improved thermal insulation effect of this feature is also aided by the less serrated nature of the more connected surface formed during heating due to SEM analysis (Fig. 8) and verified by FTIR absorbance measurements (Fig. 7). Based on the thermographic evidence, it is firmly established that SZG coating not only offers passive infrared camouflage but also acts proactively to cover the heat radiation there is and therefore, it is most suited as thermal protection and stealth capability in aerospace or any high temperature industrial application.

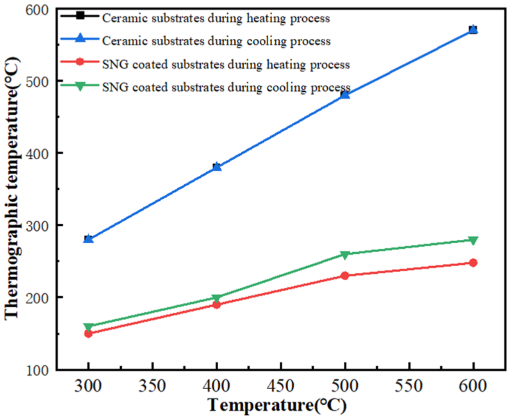

Fig. 11 Infrared radiation temperature of SZG coating.

Figure 11 depicts the comparison of the change in temperature of the infrared radiation of the bare ceramic substrates and of the SZG-coated substrates in the process of heating up and cooling down. The lack of coating on the ceramic leads to a linear relationship between surface thermographic temperatures and furnace setpoint of the order of 590° C at 600 ° C, so surface infrared emissivity is high (~0.95), and radiative heat flux opposes cooling. In the SZG coated substrates, on the other hand, the thermal radiation is largely diminished, as is evident in the apparent surface temperatures, which could not be above 300° C at a furnace of 600° C. It is through this low emissivity of the SZG coating and enhanced reflectivity of the surface post thermal treatments that we get this significant reduction in radiative temperature. Red and green data lines that define the coated sample reflect the plateau part of the temperature above which 500 ° C is an example, leading to thermal saturation and crossing to the reflection domination on the top as opposed to emission. The subdued radiation signature of the coated substrate emphasizes the fact that it has shown better results in reducing emissivity in the mid-IR range, which is important in terms of infrared camouflage and heat shielding. The hysteresis effect between the heating and cooling reversals is significantly lower with the SZG sample as compared to the uncoated ceramic, yet another indication of its capability to buffer the flux of heat and sustained emissive behavior. The graph is a quantitative verification of the thermographic views in Figure 10, containing the infrared display of the observations, which help to support the practical efficiency of the composite design scheme.

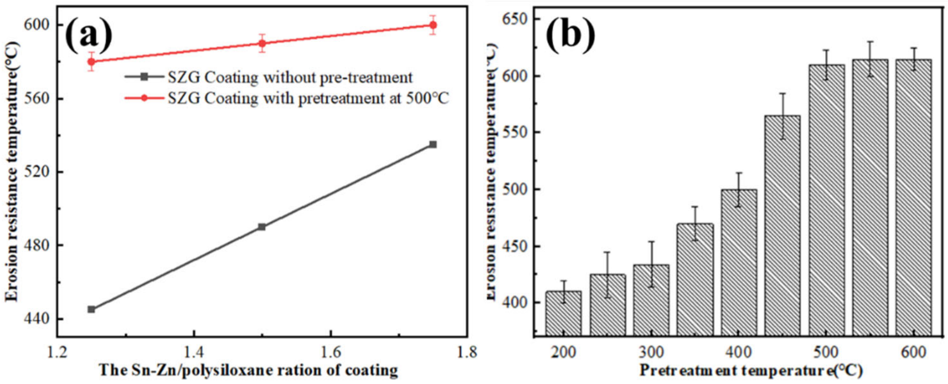

Fig. 12 (a) The WER temperature of the different SZ powders /polysiloxane ratio coatings (b) the WER temperature of the SZG coatings with different pretreatment temperatures.

In Figure 12, the temperature profile of wind erosion resistance (WER) of SZG coating is demonstrated, and the impact of pre-treatment and compositions is shown. Figure (a) shows that the erosion resistance of coatings containing different amounts of Sn-Zn/polysiloxane mass ratios is linear across temperatures of ~450 to ~520 ° C without any pretreatment, which shows that the coatings with more content of metal filler are more structurally stable against the thermal and mechanical strains. Nevertheless, pre-threading at 500 ° C displays the ALL compositions having much better WER temperatures approaching 600 ° C, with a reduced dependence on filler amount, implying that the pretreatment thermal pre-conditioning may predominate in stabilizing the coating microstructure. Panel (b) also looks into the temperature effect on resistance to erosion in the pretreatment. Such behaviour can be related to a successive breakdown of the polysiloxane network, recrystallization and viscous flow of the B2O3-SiO2-Bi2O3 glassy phase, and crystalline regrowth-fusing of Sn-Zn alloy particles --(which all contribute to filling of the pores, healing of the interfaces, and packing of the surface). These results and conclusions demonstrate that thermal pretreatment at approximately 500 ° C is keen on activating synergistic morphological evolution of the SZG coating, which has led to improved high-temperature erosion defence capability.

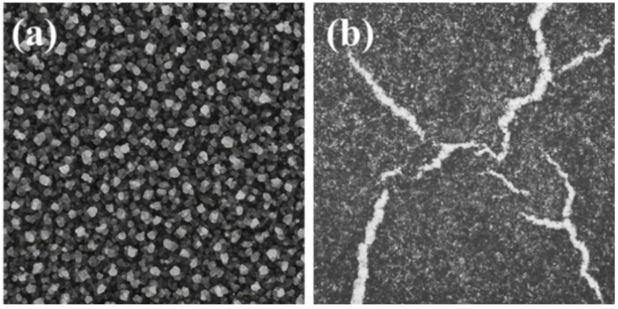

Fig. 13 Morphologies of the SZG coatings after being tested by the wind erosion at 600°C. Coatings pretreated at (a) 500 and (b) 400°C.

Fig. 13 Morphologies of the SZG coatings after being tested by the wind erosion at 600°C. Coatings pretreated at (a) 500 and (b) 400°C.

In Figure 13, the wind erosion efficiency of post-tests of SZG erosion-resistant coatings seeded at 600 ° C is given, subjected to an antecedent temperature of 400 ° C (a) and a pretreatment temperature of 500 ° C (b), respectively. The coating surface prepared at 500 ° C in panel (a) is still dense, uniform, and devoid of any cracks. The densely filled microstructure ascertains that structural transformations, viz. polysiloxane collapse, alloy remodelling of Sn and Zn, as well as softening of B2O3-SiO2-Bi2O3 glass, were fully mobilised in pretreatment. It has been observed that this damage was caused by incompletely degraded polysiloxane and extremely low glass phase flows that lead to considerable strain residue upon rapid heating and impacts, leading to gas under. Strong bonding and homogeneity among the filler particles are lacking; thus, the bonding between the particles is easily displaced in the event of a wind erosion test. This direct visual evidence supports the quantitative WER data plotted in Fig. 12, and it fully supports the point presented earlier that pretreatment at ~500 ° C is indeed paramount to the realisation of erosion resistance. The measured results underline the necessity of coinciding thermal development of all layers of coating to reach the following objectives: preventing the formation of cracks, maintaining mechanical strength, and operational sustainability even when operating in environments with high temperatures in the fluids. An optimised pretreatment procedure is therefore one of the major methods of boosting the performance of coatings in real-life thermal protection systems.

4. Conclusion

This research has proposed a multifunctional low-infrared-emissivity polysiloxane resin-based coating system that consists of Sn-Zn alloy powder (70:30) and B2O3-SiO2-Bi2O3 glass powder, and systematically researched it. A variety of thermal, morphological, infrared, and mechanical analyses were used to prove that synergistic thermal development of organic and inorganic materials is essential to attaining optimal performance when exposed to high temperatures. The TA demonstrated that the eutectic melting point of Sn-Zn alloy is very low (~360° C), which indicates that the early rearrangement and densification of the surface occur at the low stages. At the same time, the multicomponent BSB glass is softened within 380-520 ° C, being able to fill pores and resulting in the strong bonding between particles. Their co-evolution occurs in the thermo treatment of the coating or when the temperature has been pre-heated to 500 ° C. SEM imagery of the microstructural change and FTIR reflectance spectra also attested the fact that the 500 ° C treater coating generates a much denser and smoother surface that increases infrared reflection and lowers emissivity. Infrared thermographic experiments proved that the coating was able to reduce surface radiations, and this can be measured up to 250 300 degrees Celsius compared to unprotected ceramic-based surfaces at temperatures of 600 degrees Celsius. Moreover, wind erosion resistance (WER) testing resulted in further evidence of the thermal-mechanical durability of coatings pre-treated at 500 ° C, as thermal-mechanical durability was highest, reaching temperatures of 600 ° C before the cracks formed. On the contrary, coatings that were cured below this temperature were severely cracked and exhibited interfacial failure. In general, the ability of the SZG coating to exhibit infrared stealthiness, thermal stability, and erosion resistance is superior. The understanding that was obtained in this work gives a sound basis to understand the design of newer-generation thermal protective and stealth coatings in the field of aerospace, military, and energy. Future advanced high-temperature functional integration will be founded upon a change to the structure of the filler to optimize further the filler architecture and the study of multilayered gradient structures.

References

[1] Zhuang, Y., W. Zhang, and Q. Zhang, Preparation and characterization of high-performance composite coatings compatible with near-infrared low reflectivity and low infrared emissivity. Coatings, 2023. 13(12): p. 2033

[2] Yuan, L., et al., Effects of shape, size and solid content of Al pigments on the low-infrared emissivity coating. Materials Research Innovations, 2015. 19(sup1): p. S1-325-S1-330.

[3] Setien-Fernández, I., et al., First spectral emissivity study of a solar selective coating in the 150–600 C temperature range. Solar energy materials and solar cells, 2013. 117: p. 390-395.

[4] Mahfouz, L., et al., Thermal Barrier Coatings in burner rig experiment analyzed through LAser Shock for DAmage Monitoring (LASDAM) method. Journal of the European Ceramic Society, 2024. 44(13): p. 7867-7882.

[5] Xu, C., X. Wang, and J. Liu, Spinel Cu–Mn–Cr oxide nanoparticle-pigmented solar selective coatings maintaining> 94% efficiency at 750° C. ACS Applied Materials & Interfaces, 2022. 14(29): p. 33211-33218.

[6] Leng, K., et al., Multilayer GZ/YSZ thermal barrier coating from suspension and solution precursor plasma spray. Ceramics International, 2024. 50(1): p. 631-649.

[7] He, X., et al., High emissivity coatings for high temperature application: Progress and prospect. Thin Solid Films, 2009. 517(17): p. 5120-5129.

[8] Qi, L., et al., Effects of low-melting glass powder on the thermal stabilities of low infrared emissivity Al/polysiloxane coatings. Progress in Organic Coatings, 2020. 142: p. 105579.

[9] Xu, C.-A., et al., Study on the surface properties and thermal stability of polysiloxane-based polyurethane elastomers with aliphatic and aromatic diisocyanate structures. Colloid and Polymer Science, 2020. 298(9): p. 1215-1226.

[10] Qi, L., et al., Effect of high-temperature compositional and structural evolution of the polysiloxane coating with glass/Al powder on the infrared and mechanical properties. Polymer Degradation and Stability, 2023. 215: p. 110461.

[11] Fang, K., Y. Zhao, and F. Fang, Infrared stealth nanofibrous composite with thermal stability and mechanical flexibility. Journal of Alloys and Compounds, 2021. 855: p. 157418.

[12] Wang, Y., et al., In situ integration of high-temperature thin-film sensor for precise measurement of heat flux and temperature on superalloy substrate. IEEE Sensors Journal, 2023. 23(16): p. 17932-17941.

[13] Khurana, N., et al. Effect of Radiation on Polymeric Binder for Development of Radiation Resistant Coating. in Macromolecular Symposia. 2025. Wiley Online Library.

[14] Qi, L., et al., Improved thermal expansion performance of Aluminum/polysiloxane/glass coatings with low infrared emissivity by zinc powder. Infrared Physics & Technology, 2020. 110: p. 103458.